

Geometric and Electronic Structures of Terbium–Silicon Mixed Clusters (TbSi_n ; $6 \leq n \leq 16$)

M. Ohara,[†] K. Miyajima,[†] A. Pramann,[†] A. Nakajima,^{*,†} and K. Kaya[‡]

Keio University, Faculty of Science and Technology, Department of Chemistry, 3-14-1 Hiyoshi, Kohoku-ku, Yokohama 223-8522, Japan, and Institute for Molecular Science, Myodaiji, Okazaki 444-8585, Japan

Received: August 1, 2001; In Final Form: November 12, 2001

The geometric and the electronic structures of terbium–silicon anions, TbSi_n^- ($6 \leq n \leq 16$) were investigated by using photoelectron spectroscopy (PES) and a chemical-probe method. The clusters were produced by a double-rod laser vaporization technique. From trends observed in the electron affinities (EAs), the TbSi_n^- clusters were categorized into three groups of (I) $6 \leq n \leq 9$, (II) $n = 10, 11$, and (III) $n \geq 12$. Together with adsorption reactivity toward H_2O it is concluded that a Tb atom is encapsulated inside a Si_n cage at $n \geq 10$; Tb@Si_n .

I. Introduction

Small silicon clusters have been extensively investigated both experimentally and theoretically,^{1–9} because silicon is a semiconductor element of great importance in the microelectronics industry. Recently, it was reported that Si_n cage clusters with a transition metal atom trapped on the inside of Si_n ; M@Si_n ($\text{M} = \text{metal}$) act as a tunable building block of new materials.¹⁰ In addition to the silicide clusters, silicon nanocrystals have also shown large application potential in optoelectronics,^{11–16} and have been widely studied. In particular, the intense 1540 nm photoluminescence observed from erbium (Er)-doped nanocrystalline Si thin films has aroused interest in lanthanide-doped Si nanocrystals.^{17–24}

Although it is very significant to explore efficient novel light-emitting materials, neither details of emission mechanism nor crystalline structures of the lanthanide-atom-doped silicon system are known. Microscopic knowledge of the geometric and electronic structures for lanthanide–silicon binary clusters is very important for fundamental understanding of the emission mechanism and also for developing a promising way to design optoelectronic materials by cluster assembly. Especially, the formation of Ln@Si_n ($\text{Ln} = \text{lanthanide}$) clusters is fascinating because it can be regarded as a novel minimum unit for a molecular device.

In this study, we study the geometric and the electronic structures of Si_n clusters with one terbium (Tb) atom (a lanthanide) by measuring the mass spectra, the adsorption reactivities, and photoelectron spectra for the cluster anions.

II. Experimental Section

Details of both experimental setups of the chemical adsorption experiment, and photoelectron spectroscopy have been described in detail elsewhere.²⁵ In brief, the binary clusters were produced by the double rod laser vaporization technique. Both the Si and the Tb rods were independently vaporized by means of two frequency-doubled Nd^{3+} :YAG lasers. The vaporized Si and Tb atoms were cooled to room temperature with a high-pressure

He carrier gas (10 atm) and then grew into Tb–Si mixed clusters. Here the Tb rod was located upstream, while the Si rod was located downstream. However the exchange of the rod position resulted in no change in the mass distribution of the binary clusters.

To obtain information on the geometric structure of the binary clusters, adsorption reactivity for the clusters was measured by using a flow-tube reactor (FTR) combined with the cluster source. Water vapor diluted with 1.5 atm of He gas was used as the reactant gas, and was injected into FTR. The binary clusters were synchronously mixed with the reactant gas pulse at FTR, and reacted with the reactant molecule. After the cluster beam was skimmed, the anion clusters were accelerated to 3 keV with a pulsed electric field, and were mass-analyzed by a time-of-flight (TOF) mass spectrometer equipped with a reflectron. To measure the relative adsorption reactivity for the clusters, mass spectra of the cluster anions were measured before and after the reaction.

In the photoelectron spectroscopy measurements of the mixed cluster anions, the clusters were accelerated to 900 eV. After the ions were mass-selected, a pulsed electric decelerator considerably reduced their kinetic energy before they entered the photodetachment region of a magnetic-bottle-type electron spectrometer. Then the fourth harmonic (266 nm, 4.66 eV) of a pulsed Nd^{3+} :YAG laser was focused onto the mass-selected clusters to detach photoelectrons. The electrons were guided by a strong inhomogeneous magnetic field and subsequently with a weak guiding magnetic field, and detected by a microchannel plate (MCP). Their kinetic energy was analyzed by their TOF. The photoelectron signal was typically accumulated to 20000–40000 shots.

III. Results and Discussion

III.1. Geometric Structures of TbSi_n^- Clusters. Figure 1, parts a and b, show typical mass spectra of the Tb–Si binary cluster anions before and after exposure to H_2O , respectively. Peaks of the mixed clusters are labeled by solid-triangles (\blacktriangle) and bare clusters by (\bullet). Spectrum (a) shows Si_n^- clusters with one Tb atom for $n = 6–16$.

As clearly seen in Figure 1b, TbSi_n^- clusters at $n = 6–9$ decrease upon reaction toward H_2O gas, while the clusters with

* Author to whom correspondence should be addressed. E-mail: nakajima@sepia.chem.keio.ac.jp.

[†] Keio University.

[‡] Institute of Molecular Science.

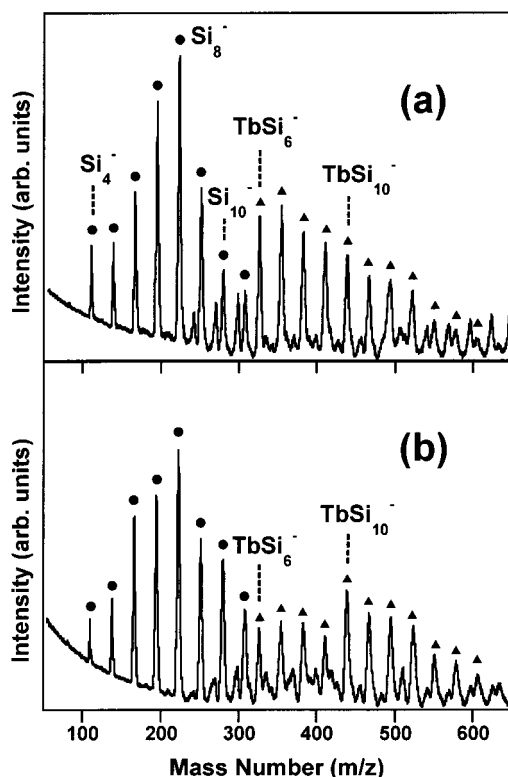


Figure 1. Time-of-flight mass spectra of Tb–Si binary cluster anions, (a) before and (b) after adsorption reaction with H_2O . In the spectra (a) and (b), peaks of pure Si clusters and Tb–Si binary clusters are labeled by the solid-circles (\bullet) and the solid-triangles (\blacktriangle), respectively.

$n = 10$ – 16 remain unchanged. It is reasonable to presume that an exterior Tb atom is a reactive site for the adsorption reaction of TbSi_n^- clusters at $n = 6$ – 9 , because it has been known that the reactivity of a lanthanide atom toward H_2O is high, and the lanthanide atoms react with H_2O to form lanthanides–hydroxides/oxides charge-transfer complexes. In contrast, the reactivities of pure Si_n^- clusters are extremely low toward the reactant molecules in comparison with the lanthanide atom. After the adsorption reaction, indeed, no significant decrease of the peak intensities for the pure Si_n^- clusters was observed. The low reactivity of TbSi_n^- at $n = 10$ – 16 toward H_2O indicates that the clusters have no exterior Tb atom. Thus, presumed geometric structures of them are cage structures with a Tb atom trapped on the inside of Si_n clusters; Tb@Si_n . In other words, 10 Si atoms are necessary at least to surround one Tb atom with a close-packed structure.

A similar M@Si ($\text{M} = \text{metal}$) cage structure has already been found in “transition metal–silicon” mixed clusters. In case of “tungsten (W)–silicon” binary clusters, the smallest cluster size of a caged WSi_n cluster is observed to be W@Si_{10} by Sanekata et al.,²⁶ to be W@Si_{12} by Kanayama and co-workers,¹⁰ and to be W@Si_{15} by Beck, depending on production methods.²⁷ These results imply that it is possible to cover one Tb atom with a caged Si_{10} cluster, providing sufficient interstitial space, although the volume of a Tb atom is slightly larger than that of a W atom (the metallic bond radii of a W atom and a Tb atom are about 1.37 and 1.78 Å, respectively.²⁸) Furthermore, the existence of caged TbSi_{10} clusters is also supported in terms of a bulk silicon crystal doped with a metal atom. When a metal atom (e.g., transition metal atom) diffuses into the silicon lattice, it can occupy an interstitial site in the lattice.^{29,30} The tetrahedral interstitial site in the silicon crystal has 4 nearest neighbor atoms and 6 next nearest neighbor atoms for a total coordination of 10 atoms (see Figure 1b of ref 31 or Figure 1 of ref 4a). This

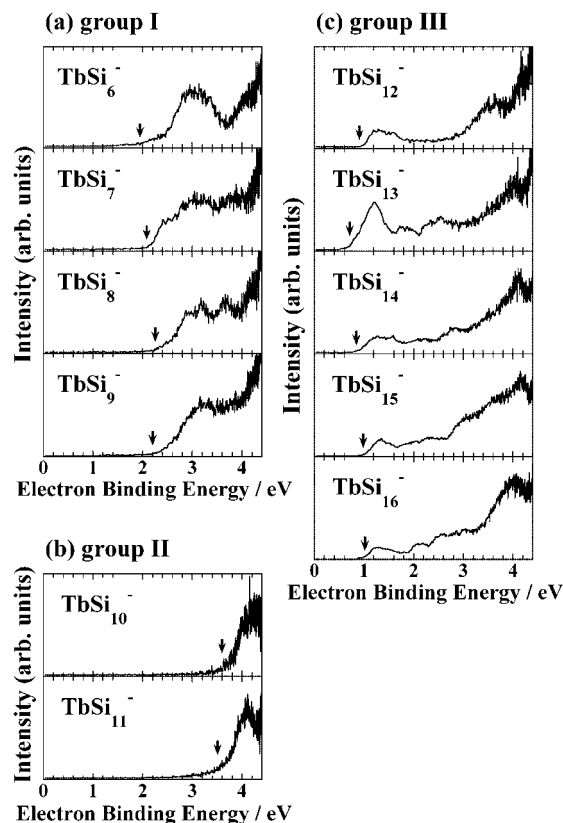


Figure 2. Photoelectron spectra of TbSi_n^- ($n = 6$ – 16) measured at a photon energy of 4.66 eV (266 nm). (a) $n = 6$ – 9 (group I), (b) $n = 10$, 11 (group II), and (c) $n = 12$ – 16 (group III). The downward arrows indicate threshold energies, corresponding to electron affinities.

coordination number suggestively correlates with the smallest cluster size of Tb@Si_n clusters.

As mentioned above, the geometric structures of TbSi_n^- clusters were presumed by using the chemical probe method. Although it is expected that some adducts were produced by the adsorption reaction, they were not observed in the mass spectrum (see Figure 1b). In some adsorption reactions, indeed, some adduct peaks have been observed in the mass spectrum.^{25a} However, most of the adducts have been observed as the cluster cations. Note in this study, we have examined the relative adsorption measurement for the cluster anions. For the cluster anions, it is generally difficult to observe the adducts in the anion mass spectrum, because electron detachment is a main process for stabilizing the adducts formed through an exothermic reaction.³² Thus, most adducts produced by the adsorption reaction result in neutral species, which are not observed in the anion mass spectrum.

III.2. Photoelectron Spectra of TbSi_n^- ($n = 6$ – 16). To reveal electronic structures of these clusters, we measured the photoelectron spectra of these cluster anions. Photoelectron spectroscopy for cluster anions is a powerful technique to investigate the electronic and geometric structure of clusters with size selection.

Figure 2 shows photoelectron spectra of TbSi_n^- ($n = 6$ – 16) at 266 nm. To obtain the threshold detachment energy (E_T) which corresponds to the upper limit of adiabatic electron affinity (EA), the slope of the first onset was extrapolated linearly to the baseline of the spectrum. A downward arrow indicates the position of E_T in each spectrum. The values of EAs are listed in Table 1. From the spectral features, TbSi_n^- clusters at $n = 6$ – 16 were categorized roughly into three groups: $n = 6$ – 9 , $n = 10$, 11, and $n = 12$ – 16 . TbSi_n^- clusters

TABLE 1: Electron Affinities of TbSi_n and Si_n Clusters in eV

	cluster size <i>n</i>	TbSi _n	Si _n
(a) Group I	6	1.95	1.8 ^a
	7	2.08	1.7 ^a
	8	2.23	2.3 ^a
	9	2.20	2.4 ^a
(b) Group II	10	3.60	2.2 ^a
	11	3.55	2.5 ^a
(c) Group III	12	0.91	2.6 ^a
	13	0.70	3.2 ^b
	14	0.84	3.2 ^b
	15	0.98	3.1 ^b
	16	1.01	3.2 ^b

^a Ref 2. ^b Ref 33.

at $n = 6-9$ are categorized as “group I” having EAs around 2.1 eV. TbSi₁₀ and TbSi₁₁ correspond to “group II” having EAs around 3.6 eV, and TbSi_n clusters at $n = 12-16$, having low EAs of 1.0 eV, are “group III”.

Photoelectron spectra of pure Si_n⁻ clusters at 266 nm have been reported and their EAs have been determined.^{2,33} EAs of Si_n at $n = 6-16$ are also listed in Table 1 in order to compare with that of TbSi_n. EAs of Si_n and TbSi_n are almost the same at $n = 6-9$ (group I). As mentioned in the preceding section, TbSi_n ($n = 6-9$) clusters presumably consist of the Si_n clusters and the exterior Tb atom. It is possible to presume that the observed electron was detached from either a Si-localized orbital or Tb-localized orbital. Here, it seems a reasonable expectation that Tb-Si_n clusters are formed through ionic bonding, distributing valence electrons of the Tb atom into the Si_n clusters, because most of the lanthanide complexes are well-known as charge-transfer complexes where the lanthanide atoms are positively charged. Thus, it is implied to transfer a 6s electron of the Tb atom to the singly occupied molecular orbital (SOMO) of pure Si_n⁻ clusters, resulting in a configuration of Tb¹⁺Si_n²⁻. This reasonably explains the similarity between EAs of TbSi_n and pure Si_n. Namely, the electron-detachment occurs from the highest occupied molecular orbital (HOMO) of Si_n²⁻ clusters (corresponds to the lowest unoccupied molecular orbital (LUMO) of Si_n clusters) in TbSi_n⁻ clusters. However, we cannot exclude the contribution of the electron detachment from a Tb atom in this work. To understand the molecular orbital of the clusters more clear, a support by theoretical calculation is needed.

As shown in Figure 2, the EAs greatly increase to around 3.6 eV at TbSi₁₀. The high EA was observed also at TbSi₁₁, although TbSi₁₀⁻ seems slightly more stable than TbSi₁₁⁻ in EAs. As shown by low reactivity of these clusters toward H₂O, both the Tb atoms in TbSi₁₀ and TbSi₁₁ should be located in the caged Si clusters; Tb@Si_n. Therefore this drastic change in EAs can also be explained according to the geometric change into the caged structure. Through the Coulomb interaction with central cationic Tb atom, the hollow Si_n cage seemingly becomes electron deficient, which results in a high EA of Tb@Si_n. In addition, delocalization of the electrons would occur on the cage, and the delocalization results in high electron affinity of Tb@Si_n. Namely, the high EA observed in Tb@Si₁₀ and Tb@Si₁₁ is due to Coulomb interaction with the centered Tb cation and delocalization of the electrons on the cage, although a theoretical support is needed.

As mentioned in the preceding section, both TbSi₁₁ and TbSi₁₂ consist of the Si cage cluster and the interior Tb atom. Surprisingly, however, EA drastically drops to around 1.0 eV at $n = 12$, and the trend of low EAs is kept at $n = 12-16$ (group III). The EA drop of more than 2 eV from $n = 11$ to 12

causes either stabilization of neutral TbSi₁₂ or destabilization of anionic TbSi₁₂⁻. Since low EA is widely observed for various cluster sizes of $n = 12-16$ for TbSi_n, it seems reasonable that the EA drop should not result from any particular geometric or electronic stabilization. Namely, the EA drop should be attributed to the destabilization in the anions rather than the stabilization in the neutrals. It seems plausible that the destabilization observed between Tb@Si₁₁ and Tb@Si₁₂ is due to a considerable distortion of the caged Tb@Si_n ($n \geq 12$), although we cannot give a concrete picture for this distortion in the present stage.

IV. Conclusions

Terbium-silicon binary clusters anions, TbSi_n⁻, were produced by a double-laser vaporization method. To presume the geometric structure of TbSi_n, the chemical probe method was employed, and the adsorption reactivity of these clusters was measured toward H₂O. The high reactivity of TbSi_n⁻ at $n = 6-9$ indicated that the geometric structures of the clusters are of Tb-exterior type (a Tb atom is located on the surface of the Si_n cluster). Since the reactivity of TbSi_n⁻ at $n = 10-16$ was low in contrast, the structures of their clusters were presumed to be Tb-interior type (a Tb atom is located in the caged Si_n cluster; Tb@Si_n). The size-dependence of their EAs measured by anion photoelectron spectroscopy has revealed that the TbSi_n clusters were categorized into three groups of (I) $6 \leq n \leq 9$, (II) $n = 10, 11$, and (III) $n \geq 12$. The high EAs observed in Tb@Si₁₀ and Tb@Si₁₁ are presumably ascribed to Coulomb interaction with the centered Tb cation and delocalization of the electron on the cage. Both the results of the adsorption reactivity and the photoelectron spectroscopy for TbSi_n⁻ clusters indicated that the smallest Tb@Si_n cluster is Tb@Si₁₀.

Acknowledgment. This work is supported by a program entitled “Research for the Future (RFTF)” of the Japan Society for the Promotion of Science (98P01203). M.O. expresses gratitude to Research Fellowships of the Japan Society for the Promotion of Science for Young Scientists.

References and Notes

- (1) Brown, W. L.; Freeman, R. R.; Raghavachari, K.; Schluter, M. *Science* **1987**, 235, 860.
- (2) Cheshnovsky, O.; Yang, S. H.; Pettiette, C. L.; Craycraft, M. J.; Liu, Y.; Smaller, R. E. *Chem. Phys. Lett.* **1987**, 138, 119.
- (3) (a) Kitsopoulos, T. N.; Chick, C. J.; Weaver, A.; Neumark, D. M. *J. Chem. Phys.* **1990**, 93, 6108. (b) Kitsopoulos, T. N.; Chick, C. J.; Zhao, Y.; Neumark, D. M. *ibid.* **1991**, 95, 1441. (c) Arnold, C. C.; Kitsopoulos, T. N.; Neumark, D. M. *ibid.* **1993**, 99, 766. (d) Arnold, C. C.; Neumark, D. M. *ibid.* **1993**, 99, 3353. (e) Arnold, C. C.; Neumark, D. M. *ibid.* **1994**, 100, 1797.
- (4) (a) Jarrold, M. F. *Science*. **1991**, 252, 1085. (b) Jarrold, M. F.; Honea, E. C. *J. Phys. Chem.* **1991**, 95, 9181.
- (5) Fuke, K.; Tsukamoto, K.; Misaizu, F.; Sanekata, M. *J. Chem. Phys.* **1993**, 99, 7807.
- (6) Honea, E. C.; Ogura, A.; Murray, C. A.; Raghavachari, K.; Sprenger, W. O.; Jarrold, M. F.; Brown, W. L. *Nature (London)* **1993**, 366, 42.
- (7) (a) Raghavachari, K.; Logovinsky, V. *Phys. Rev. Lett.* **1985**, 55, 2853. (b) Raghavachari, K. *J. Chem. Phys.* **1986**, 84, 5672. (c) Raghavachari, K.; Whiteside, R. A.; Pople, J. A. *ibid.* **1986**, 85, 6623. (d) Raghavachari, K.; Binkley, J. S. *ibid.* **1987**, 87, 2191. (e) Raghavachari, K.; Rohlffing, C. M. *ibid.* **1988**, 89, 2219. (f) Raghavachari, K.; Rohlffing, C. M. *ibid.* **1991**, 94, 3670. (g) Rohlffing, C. M.; Raghavachari, K. *ibid.* **1992**, 96, 2114.
- (8) von Niessen, W.; Zakrewski, V. G. *J. Chem. Phys.* **1993**, 98, 1271.
- (9) Ho, K.-M.; Shvartsburg, A. A.; Pan, B.; Lu, Z.-Y.; Wang, C.-Z.; Wacker, J. G.; Fye, J. L.; Jarrold, M. F. *Nature (London)* **1998**, 392, 582.
- (10) Hiura, H.; Miyazaki, T.; Kanayama, T. *Phys. Rev. Lett.* **2001**, 86, 1733.
- (11) Lyer, S. S.; Xie, Y. H. *Science* **1993**, 260, 40.

- (12) (a) Kanematsu, Y.; Uto, H.; Masumoto, Y.; Matsumoto, T.; Futagi, T.; Mimura, H. *Phys. Rev. B* **1993**, *48*, 2827. (b) Kanematsu, Y.; Ogawa, T.; Shiraishi, K.; Takeda, K. *ibid.* **1993**, *48*, 4883.
- (13) (a) Prokes, S. M.; Glembocki, O. J. *Phys. Rev. B* **1994**, *49*, 2238. (b) Prokes, S. M.; Carlos, W. E.; Glembocki, O. J. *ibid.* **1994**, *50*, 17093.
- (14) Veprek, S.; Ruckschiess, M.; Wirschem, Th.; Landkammer, B. *Appl. Phys. Lett.* **1995**, *67*, 2215.
- (15) Hirschman, K. D.; Tsybeskov, L.; Dutttagupta, S. P.; Fauchet, P. M. *Nature (London)* **1996**, *384*, 338.
- (16) Cullis, C. A.; Canham, L. T.; Calcott, P. D. J. *J. Appl. Phys.* **1997**, *82*, 909.
- (17) (a) Fujii, M.; Yoshida, M.; Hayashi, S.; Yamamoto, K. *J. Appl. Phys.* **1998**, *84*, 4525. (b) Fujii, M.; Yoshida, M.; Kanzawa, Y.; Hayashi, S.; Yamamoto, K. *Appl. Phys. Lett.* **1997**, *71*, 1198.
- (18) Zhao, X. Z.; Komura, S.; Isshiki, H.; Aoyagi, Y.; Sugano, T. *Appl. Phys. Lett.* **1999**, *74*, 120.
- (19) Komura, S.; Katsumata, T.; Morikawa, T.; Zhao, X.; Isshiki, H.; Aoyagi, Y. *Appl. Phys. Lett.* **1999**, *74*, 377.
- (20) Chryssou, C. E.; Kenyon, A. J.; Iwayama, T. S.; Pitt, C. W.; Hole, D. E. *Appl. Phys. Lett.* **1999**, *75*, 2011.
- (21) Franzo, G.; Pacifici, D.; Vinciguerra, V.; Priolo, F. *Appl. Phys. Lett.* **2000**, *76*, 2167.
- (22) (a) Kik, P. G.; Brongersma, M. L.; Polman, A. *Appl. Phys. Lett.* **2000**, *76*, 2325. (b) Kik, P. G.; Polman, A. *J. Appl. Phys.* **2000**, *88*, 1992.
- (23) Priolo, F.; Franzo, G.; Pacifici, D.; Vinciguerra, V.; Iacona, F.; Irrera, A. *J. Appl. Phys.* **2001**, *89*, 264.
- (24) Wu, X. L.; Mei, Y. F.; Siu, G. G.; Wong, K. L.; Moulding, K.; Stokes, M. J.; Fu, C. L.; Bao, X. M. *Phys. Rev. Lett.* **2001**, *86*, 3000.
- (25) (a) Nakajima, A.; Kaya, K. *J. Phys. Chem. A* **2000**, *104*, 176. (b) Nakajima, A.; Taguwa, T.; Hoshino, K.; Sugioka, T.; Naganuma, T.; Ono, F.; Watanabe, K.; Nakao, K.; Konishi, Y.; Kishi, R.; Kaya, K. *Chem. Phys. Lett.* **1993**, *214*, 22.
- (26) Sanekata, M.; Koya, T.; Nagao, S.; Negishi, Y.; Nakajima, A.; Kaya, K. *Trans. Mater. Res. Soc. Jpn.* **2000**, *25* (4), 1003.
- (27) (a) Beck, S. M. *J. Chem. Phys.* **1987**, *87*, 4233. (b) Beck, S. M. *ibid.* **1989**, *90*, 6306.
- (28) Emsley, J. *The Elements*; Oxford University Press: New York, 1989.
- (29) Woodbury, H. H.; Ludwig, G. W. *Phys. Rev.* **1960**, *117*, 102.
- (30) Ludwig, G. W.; Woodbury, H. H. *Solid State Phys.* **1962**, *13*, 223.
- (31) Beck, S. M. *Photophysical studies of Bare and Metal-Containing Silicon Clusters, ADVANCES IN METAL AND SEMICONDUCTOR CLUSTERS*; JAI PRESS INC: London, 1993.
- (32) Nakajima, A.; Hayase, T.; Hayakawa, F.; Kaya, K. *Chem. Phys. Lett.* **1997**, *280*, 381.
- (33) Maus, M.; Gantefor, G.; Eberhardt, W. *Appl. Phys. A* **2000**, *70*, 539.